Complex conductivity of high-T_c single crystals in the microwave band: Some intermediate results and unsolved problems

M. R. Trunin
Institute of Solid State Physics RAS, 142432 Chernogolovka, Moscow district, Russia
(March 14, 2001)

The analysis of investigations of the microwave surface impedance $Z_s(T)$ and conductivity tensor $\hat{\sigma}(T)$ of HTS single crystals as functions of temperature, alongside the procedure of their derivation from parameters measured directly in experiments, has revealed a number of facts that contradict previously developed electrodynamic models of the conductivity in these materials. The paper is dedicated to plausible causes of these discrepancies, which are assumed to be related to specific features of HTS structures, and to particular questions that should be answered by the research undertaken in the immediate future, among which the major problem is the nature of residual losses in HTS.

I. INTRODUCTION

Microwave measurements of the temperature dependence of the complex conductivity $\hat{\sigma}(T)=\hat{\sigma}'(T)-i\hat{\sigma}''(T)$ of high-T_c superconductors (HTS) have advanced considerably our understanding of the pairing mechanism in these materials. The real part $\hat{\sigma}'(T)$ is susceptible to the scattering rate of quasiparticles, as well as their density of states. The imaginary part $\hat{\sigma}''(T)$ is related to the magnetic field penetration depth $\lambda(T)$. Because of the high anisotropy of HTS crystals, the conductivity $\hat{\sigma}$ is a tensor characterized by its components σ_{ab} and σ_c.

The first part of this paper considers derivation of $\sigma_{ab}(T)$ and $\sigma_c(T)$ from the measured temperature dependences of the Q-factor and the frequency shift δf of the cavity for different sample alignments with respect to the ac magnetic field $\mathbf{H}_\omega$. In the local electrodynamics, which can be applied to the discussed experiments, $\hat{\sigma}(T)=i\omega\mu_0/Z_s^2(T)$, where $Z_s(T)=R_s(T)+iX_s(T)$ is the surface impedance of the sample. At microwave frequencies the imaginary part of the surface impedance, the surface reactance X_s, reflects mainly the response of the superconducting carries and is due to the nondissipative energy stored in the surface layer of the superconductor. The real part, the surface resistance R_s, is proportional to the microwave losses and is due to the normal carriers.

In the second part of the paper we will analyze the common and distinctive features of the temperature dependences of $Z_s^{ab}(T)$ and $\sigma_{ab}(T)$ in the ab-plane of various HTS single crystals. Our attention in this analysis will be focused on the magnitude of the residual losses, whose nature in HTS is, perhaps, the central topic of investigations and discussions. In addition, we will discuss a phenomenological model describing the microwave response of HTS crystals. Finally, the problem of the anisotropy in the conductivity of HTS materials will be broached.

II. MEASURED QUANTITIES AND SAMPLES

The most convenient technique for measurements of the surface impedance of small HTS samples in the X-W microwave frequency bands is the so-called 'hot-finger' method. The underlying idea of the method is that a crystal is set on a sapphire rod at the center of a superconducting cylindrical cavity resonating at the frequency f in the H_{011} mode, i.e., at the antinode of a quasi-homogeneous microwave magnetic field (Fig. 1). By varying the rod temperature, measuring the Q_s-factor and frequency shift Δf_s of the cavity with the sample inside, and comparing them with the parameters of the empty cavity, Q_e and Δf_e, one can determine the sample surface resistance R_s and reactance X_s as functions of temperature using the relations[1]

$$R_s(T)=\Gamma_s\Delta(1/Q)=\Gamma_s\left[Q_s^{-1}(T)-Q_e^{-1}(T)\right], \quad (1)$$

$$X_s(T)=-2\Gamma_s\frac{\delta f}{f}=-\frac{2\Gamma_s}{f}\left[\Delta f_s(T)-\Delta f_e(T)-f_0\right], \quad (2)$$

where $\Gamma_s=\omega\mu_0\int_V H_\omega^2 dV/[\int_S H_s^2 dS]$ is the sample geometrical factor, $\omega=2\pi f$, $\mu_0=4\pi\cdot 10^{-7}$ H/m, V is the volume of the cavity, H_ω is the magnetic field generated in the cavity, S is the total sample surface area, and H_s is the tangential component of the microwave magnetic field on the sample surface. In Eq. (1) $\Delta(1/Q)$ is the difference between the values 1/Q of the cavity with the sample inside and the empty cavity. In Eq. (2) δf is the frequency shift relative to that which would be measured for a sample with perfect screening and no penetration of the microwave fields. In the experiment we measure the difference $(\Delta f_s-\Delta f_e)=\Delta f$ between the resonant frequency shifts of the loaded and empty cavity as functions of temperature, which is equal to $\Delta f(T)=\delta f(T)+f_0$, where f_0 is a constant. The constant f_0 includes both the perfect-conductor shift and the uncontrolled contribution caused by opening and closing the cavity.

The efficiency of this method was tested in experiments with Nb samples[2]. The exponential dependence of the surface impedance in the low-temperature range and observation of a coherent peak in the real part of the microwave conductivity of Nb support the assertion that the BCS theory[3] adequately describes electromagnetic properties of conventional superconductors. Measurements of the London penetration depth λ_L, superconducting gap $\Delta(0)$, and coherence length ξ_0 in Nb were in agreement with literature data.

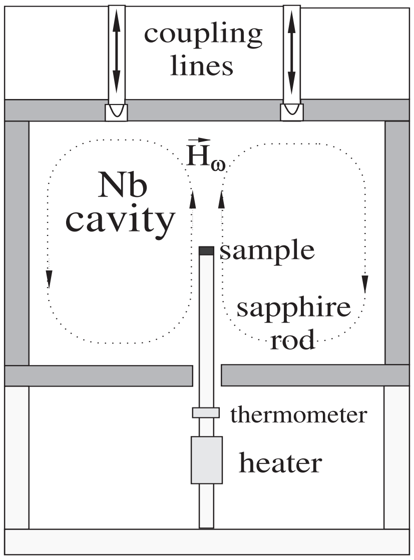

FIG. 1. Diagram of the microwave cavity used in the 'hot-finger' technique.

In this paper, we will discuss measurements of the impedance and conductivity of copper-oxide HTS single crystals, which usually have the shapes of plates with lateral dimensions $a \sim b \sim 1$ mm and thicknesses $c \sim 0.1$ mm: $YBa_2Cu_3O_{6.95}$ (YBCO, $T_c \approx 93$ K), $Bi_2Sr_2CaCu_2O_{8+\delta}$ (BSCCO #1, $T_c \approx 83$ K; BSCCO #2, $T_c \approx 92$ K), $Tl_2Ba_2CaCu_2O_{8-\delta}$ (TBCCO, $T_c \approx 112$ K), $Tl_2Ba_2CuO_{6+\delta}$ (TBCCO, $T_c \approx 90$ K). With the exception of the slightly overdoped sample BSCCO #1, the doping levels of all other samples were optimal so that their values of T_c were maximal.

Figures 2 and 3 show as examples curves of the surface resistance $R_s(T)$ and reactance $X_s(T)$ as functions of temperature measured in the ab-plane of the crystals BSCCO #1 and BSCCO #2. Equations (1) and (2) indicate that two parameters, Γ_s and f_0, are required to derive absolute values of R_s and $X_s(T)$ from measurements of $Q(T)$ and $\Delta f(T)$. The geometrical factor Γ_s depends on the shape and dimensions of the sample, and its position in the microwave cavity with respect to the microwave field $\mathbf{H}_\omega$ distribution. The parameter Γ_s can be determined both empirically and theoretically, and its value is of order of tens of kilo-ohms at a frequency ~ 10 GHz. The constant f_0 can be derived from the measurements of the microwave response of HTS single crystals in the normal state, and the determination of this parameter will be discussed in the following section.

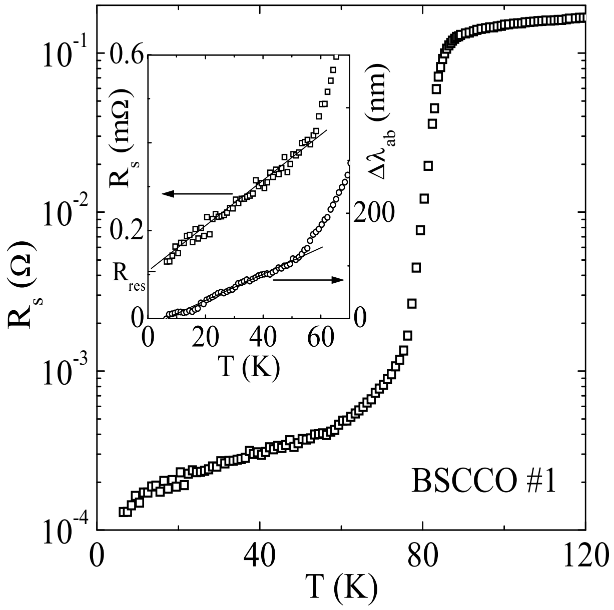

FIG. 2. Surface resistance $R_s(T)$ in the ab-plane of a BSCCO #1 single crystal at 9.4 GHz. The inset shows linear plots of $\Delta\lambda_{ab}(T)$ and $R_s(T)$ at low temperatures. The value of the residual surface resistance $R_{res} \approx 120\ \mu\Omega$ is indicated.

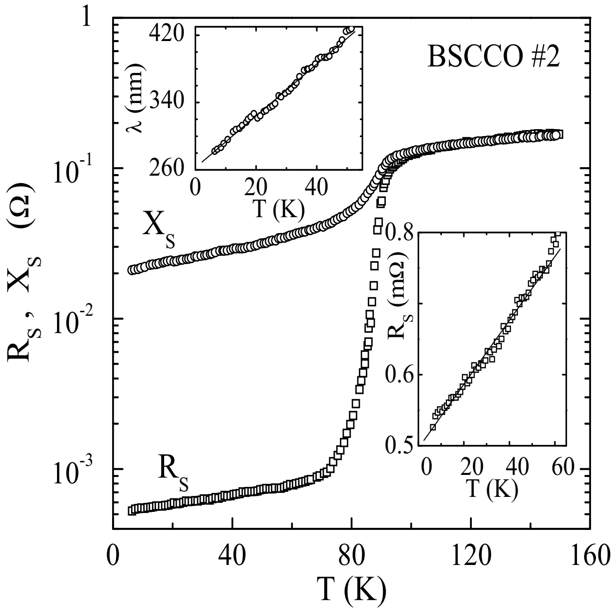

FIG. 3. Surface resistance $R_s(T)$ and reactance $X_s(T)$ in the ab-plane of a BSCCO #2 single crystal at 9.4 GHz. The insets show linear plots of $\lambda(T)$ and $R_s(T)$ at low temperatures.

Let us assess the accuracy of the surface resistance and field penetration depth determined by the hot-finger technique. The uncertainty δR_s in measurements of

$R_s(T)$, $\delta R_s = \Gamma_s \delta(Q^{-1} - Q_0^{-1}) = \Gamma_s \delta Q/Q^2$, is determined by the uncertainty $\delta Q/Q$, which was within 1% at $Q \sim 10^7$ in our experiments. If $\Gamma_s = 10$ kΩ, then we have $\delta R_s \approx 10$ $\mu\Omega$. As the temperature drops several degrees below T_c, the increment $\Delta X_s(T) = \omega\mu_0\Delta\lambda(T)$, and, given $X_s(T)$ expressed in absolute units, one can determine the magnetic field penetration depth $\lambda(T) = X_s(T)/\omega\mu_0$. The uncertainty in the relative value of the penetration depth is $\Delta\lambda(T)$, $\delta(\Delta\lambda) = (2\Gamma_s/\omega\mu_0) \cdot (\delta(\Delta\omega)/\omega)$, which equals several ångström. The error in $\lambda(T)$ can be up to 30% of the actual value $\lambda(0)$ and is largely determined by the measurement accuracy of the constant f_0.

Note also that the temperature dependence of the reactance can be notably affected by the thermal expansion of a sample. Since the resonant frequency is determined by the volume where the microwave field is confined, the thermal expansion of the sample is equivalent to a smaller penetration depth of the microwave field, and this leads to an additional frequency shift Δf_{th} in the brackets on the right of Eq. (2). It was shown in the earlier publication[1] that the contribution of $\Delta f_{th}(T)$ to the total frequency shift of the cavity with a sample inside is negligible in the range of low temperatures, however, at $T > 0.9T_c$ it may be quite considerable, especially for highly anisotropic BSCCO single crystals in the case when their ab-planes are oriented perpendicular to the microwave magnetic field $\mathbf{H}_\omega$: $\mathbf{H}_\omega \| \mathbf{c}$. In particular, the curve of $X_s(T)$ in Fig. 3 was plotted with due account of the thermal expansion of the sample BSCCO #2. Otherwise, i.e., when the thermal shift Δf_{th} in Eq. (2) is negligible, the curve of reactance, which follows that plotted in Fig. 3 up to $T \approx T_c$, has a smaller slope at $T > T_c$, and the discrepancy is 25 mΩ at $T = 150$ K.

III. CONDUCTIVITY OF ANISOTROPIC SUPERCONDUCTORS

At $T > 4$ K the relation between the electric field and current density is local in both the superconducting and normal states of HTS: $j = \hat{\sigma}E$, where the conductivity $\hat{\sigma}$ is a tensor, which is characterized by two components in the crystals with a tetragonal structure: σ_{ab} in the ab-planes of CuO_2 and σ_c in the direction perpendicular to the cuprate planes. In the normal state, an ac field penetrates in the direction of the c-axis through the skin depth $\delta_{ab} = \sqrt{2/\omega\mu_0\sigma_{ab}}$, and in the CuO_2 planes through $\delta_c = \sqrt{2/\omega\mu_0\sigma_c}$. In the superconducting state all the parameters δ_{ab}, δ_c, $\sigma_{ab} = \sigma'_{ab} - i\sigma''_{ab}$, and $\sigma_c = \sigma'_c - i\sigma''_c$ are complex. In the temperature range $T < T_c$, if $\sigma' \ll \sigma''$, the field penetration depths are given by the formulas $\lambda_{ab} = \sqrt{1/\omega\mu_0\sigma''_{ab}}$, $\lambda_c = \sqrt{1/\omega\mu_0\sigma''_c}$. In the close neighborhood of T_c, if $\sigma' \gtrsim \sigma''$, the decay of the magnetic field in a superconductor is characterized by the functions $\mathrm{Re}\,(\delta_{\rm ab})$ and $\mathrm{Re}\,(\delta_{\rm c})$, which turn to δ_{ab} and δ_c, respectively, at $T \geq T_c$.

In the hot-finger technique, the components of tensor $\hat{\sigma}$ can be derived from the measurements of the microwave response for different sample alignments with respect to the ac magnetic field $\mathbf{H}_\omega$: in the transverse (T) orientation, $\mathbf{H}_\omega \parallel \mathbf{c}$ (Fig. 4a), when the screening current flows in the ab-plane of the crystal, and in the longitudinal (L) orientation, $\mathbf{H}_\omega \perp \mathbf{c}$ (Fig. 4b), with currents running in the directions of both CuO_2 planes and the c-axis.

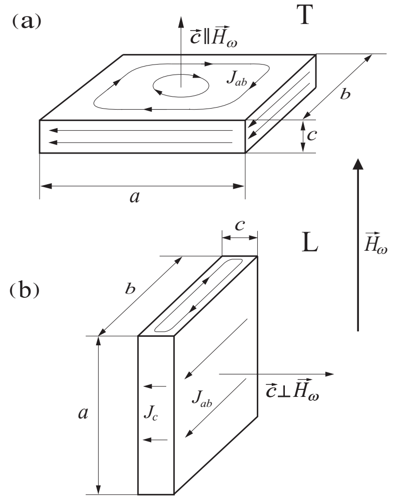

FIG. 4. (a) transverse (T) orientation of a sample with respect to microwave magnetic field, $\mathbf{H}_\omega \| \mathbf{c}$; arrows on the surfaces show directions of microwave currents; (b) longitudinal (L) orientation, $\mathbf{H}_\omega \perp \mathbf{c}$.

Let us start with the case of the T-orientation (Fig. 4a). At a frequency of ~ 10 GHz and $T \geq T_c$, the field $\mathbf{H}_\omega$ penetrates into the sample to the skin depth $\delta_{ab} \sim 5 \cdot 10^{-3}$ mm and at $T < 0.9T_c$ to the depth $\lambda_{ab} \sim 10^{-4}$ mm. Since $\lambda_{ab} \ll c$ and $\delta_{ab} \ll c$, the impedance Z_s^{ab} of the crystal in the T-orientation can be treated as a coefficient in the Leontovich boundary condition[4] at all temperatures, and the surface impedance can be related to the conductivity σ_{ab} by a local equation:

$$Z_s^{ab} = R_s + iX_s = \left(\frac{i\omega\mu_0}{\sigma_{ab}}\right)^{1/2}. \tag{3}$$

At microwave frequencies the conductivity of HTS is real if $T \geq T_c$, therefore the constant f_0 in the T-orientation in Eq. (2) is obtained, in accordance to Eq. (3), by equating the imaginary part of the impedance to the real part in the normal state, i.e., by fitting the temperature dependence $R_s(T)$ to $\Delta X_s(T)$ in the range $T \geq T_c$. In this manner $X_s(T)$ was determined over the entire range of the studied temperatures, and $\lambda_{ab}(T) = X_s(T)/\omega\mu_0$ for $T < T_c$ in Fig. 3.

In the superconducting state the conductivity σ_{ab} is complex and, as follows from Eq. (3), the real part of the surface impedance $R_s(T)$ is not equal to the imaginary part $X_s(T)$:

$$R_s(T) = \sqrt{\frac{\omega\mu_0(\varphi^{1/2}-1)}{2\sigma''\varphi}}, \quad X_s(T) = \sqrt{\frac{\omega\mu_0(\varphi^{1/2}+1)}{2\sigma''\varphi}}, \tag{4}$$

where $\varphi = 1 + (\sigma'/\sigma'')^2$. It is obvious that $R_s(T) < X_s(T)$ for $T < T_c$.

For the temperatures $T < T_c$, if $\sigma' \ll \sigma''$, Eq. (4) can be reduced to

$$R_s \simeq \frac{(\omega\mu_0)^{1/2}\sigma'}{2(\sigma'')^{3/2}} = \frac{1}{2}\omega^2\mu_0^2\sigma'\lambda^3, \quad X_s \simeq (\omega\mu_0/\sigma'')^{1/2} = \omega\mu_0\lambda. \tag{5}$$

After calculating R_s and X_s by Eqs. (1) and (2), we derive from Eq. (4) the real, σ', and imaginary, σ'', parts of the conductivity:

$$\sigma' = \frac{2\omega\mu_0 R_s X_s}{(R_s^2 + X_s^2)^2}, \quad \sigma'' = \frac{\omega\mu_0(X_s^2 - R_s^2)}{(R_s^2 + X_s^2)^2}. \tag{6}$$

An important point is that $R_s(T)$ and $X_s(T)$ should be measured in absolute units in order to determine the conductivity components from Eq. 6. Figure 5 plots $\sigma'_{ab}(T)$ and $\sigma''_{ab}(T)$ calculated with the help of Eq. (6) and characterizing the samples BSCCO #1 and BSCCO #2.

Now let us consider the case of the L-orientation of the crystal with respect to the field $\mathbf{H}_\omega$ in the cavity, namely $\mathbf{H}_\omega \perp \mathbf{c}$ (Fig. 4b). In the superconducting state, currents running in the ab-planes decay over a depth λ_{ab}, whereas those flowing in the direction of the c-axis have a penetration depth λ_c. At $T < 0.9\,T_c$ these two lengths are smaller than characteristic sample dimensions, which allows us to introduce the effective impedance Z_s^{ab+c} in the L-orientation, which is defined as an average of Z_s^{ab} and Z_s^c with the statistical weights proportional to the respective areas:

$$Z_s^{ab+c} \simeq \frac{abZ_s^{ab} + acZ_s^c}{ab + ac} = \frac{bZ_s^{ab} + cZ_s^c}{b + c}, \tag{7}$$

where the superscripts of Z_s denote the direction of the screening current. In Eq. (7) we neglect the anisotropy in the ab-planes and the contribution from the bc-faces (Fig. 4b), which is a factor $\sim c/a$ smaller than that of the ab-surfaces. Given measurements of $Z_s^{ab}(T)$ in the T-orientation and of $Z_s^{ab+c}(T)$ in the L-orientation, one can obtain the losses $R_s^c(T)$ and the change in $\Delta\lambda_c(T) = \Delta X_s^c(T)/\omega\mu_0$ from Eq. (7):

$$\Delta\lambda_c = \frac{1}{c}\left[(b+c)\,\Delta\lambda_{ab+c} - b\,\Delta\lambda_{ab}\right]. \tag{8}$$

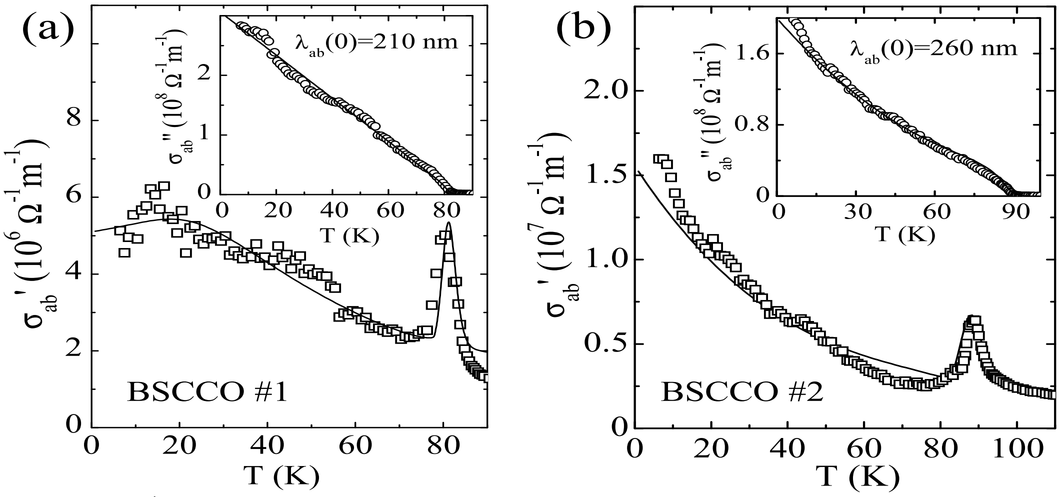

FIG. 5. Conductivities $\sigma'_{ab}(T)$ (open squares) of two BSCCO single crystals #1 (Fig. 5a) and #2 (Fig. 5b) at 9.4 GHz, extracted from the surface impedance measurements using Eq. (6). The insets show $\sigma''_{ab}(T)$ (open circles). Solid lines plot the calculations based on Eqs. (15), (17)–(19) of the modified two-fluid model with parameter $\kappa = 2$ for sample BSCCO #1 and $\kappa = 3$ for BSCCO #2 using the experimental data $T_c = 83$ K, $\delta T_c = 2.5$ K, $\omega\tau(T_c) = 7 \cdot 10^{-3}$, $\beta = 0.3$, $\alpha = 1$, $R_{res} = 120\ \mu\Omega$ for BSCCO #1 and $T_c = 92$ K, $\delta T_c = 4.5$ K, $\omega\tau(T_c) = 9 \cdot 10^{-3}$, $\beta = 2$, $\alpha = 2$, $R_{res} = 500\ \mu\Omega$ for BSCCO #2.

This technique for determination of $\Delta\lambda_c(T)$ was used in microwave experiments[5–11] at low temperatures, $T < T_c$. This method, however, does not allow us to derive $\lambda_c(T)$ from measurements of the Q-factor and shifts of the resonant frequency in the L-orientation, moreover, it cannot be applied to the range of higher temperatures. The point is that the size effect plays an important role in the L-orientation at $T > 0.9\,T_c$. Indeed, whereas the ratio $\delta_c/\delta_{ab} \sim 10$ in YBCO single crystals, and in the frequency band about 10 GHz $\delta_c \sim 0.05$ mm is comparable to the sample thickness c but less than a and b, in BSCCO, for example, this ratio can be up to 300, so that $\delta_c \sim a \sim b$. Owing to the size effect, the functional dependence of the effective parameter $R_{s,eff}^{ab+c}(T)$ measured in the normal state deviates from $\Delta X_{s,eff}^{ab+c}(T)$, as a result, one cannot determine the constant f_0 in Eq. (2) as it was done previously. In order to analyze our measurements in both the superconducting and normal states of BSCCO crystals in the L-orientation, we used the procedure[12] based on the utilization of previously known formulae for the field distribution in an anisotropic long strip ($a \gg b, c$) in the L-orientation. These formulae neglect the effect of bc-faces of the crystal if $\mathbf{H}_\omega$ is parallel to the a-edge of the crystal (Fig. 4b), but take into account the size effect. If we, following Ref.[13], introduce a complex susceptibility $\mu = \mu' - i\mu''$ defined in terms of the power $P = i\omega\mu\mu_0 H_\omega^2/2$ absorbed in the unit volume of the sample, we can replace Eqs. (1) and (2) with the formula

$$\Delta\,(1/Q) - 2i\,\delta f/f = i\gamma\mu v/V, \qquad (9)$$

which relates the measurements of $\Delta\,(1/Q)$ and $\Delta f = \delta f + f_0$ to the susceptibility $\mu(T)$. In Eq. (9) v is the volume of the sample and $\gamma = VH_0^2/[\int_V H_\omega^2 dV]$ is a constant characterizing the cavity[1]. At an arbitrary temperature, the function $\mu(T)$ in the L-orientation is controlled by the components $\sigma_{ab}(T)$ and $\sigma_c(T)$ of the conductivity tensor through the penetration depths $\delta_{ab}(T)$ and $\delta_c(T)$[12]:

$$\mu = \frac{8}{\pi^2}\sum_n \frac{1}{n^2}\left\{\frac{\tan(\alpha_n)}{\alpha_n} + \frac{\tan(\beta_n)}{\beta_n}\right\},$$

$$\alpha_n^2 = -\frac{b^2}{\delta_c^2}\left(\frac{i}{2} + \frac{\pi^2}{4}\frac{\delta_{ab}^2}{c^2}n^2\right),\ \beta_n^2 = -\frac{c^2}{\delta_{ab}^2}\left(\frac{i}{2} + \frac{\pi^2}{4}\frac{\delta_c^2}{b^2}n^2\right), \qquad (10)$$

where the sum is performed over odd integers $n > 0$. In the superconducting state at $T < 0.9\,T_c$ we find that $\lambda_{ab} \ll c$ and $\lambda_c \ll a$, and we derive from Eq. (10) a simple expression for the real part of μ:

$$\mu' = \frac{2\lambda_c}{b} + \frac{2\lambda_{ab}}{c}\ . \qquad (11)$$

One can easily check out that, in the range of low temperatures, the change in $\Delta\lambda_c(T)$ deriving from Eq. (11) is identical to that given by Eq. (8).

The advantage of the suggested approach, which takes account of the size effect, is the possibility of estimating the constant f_0 in Eq. (9), hence the real $\sigma_c'(T)$ and imaginary $\sigma_c''(T)$ components of the conductivity tensor measured along the c-axis can be determined. The procedure of determination of the constant f_0 for BSCCO #1 and BSCCO #2 single crystals is illustrated by Figs. 6a and 6b respectively. Using the measurements of $\sigma_{ab}(T)$ at $T > T_c$ in the T-orientation (Fig. 5), alongside the data on $\Delta(1/Q)$ in the L-orientation (open squares in Fig. 6), and substituting the imaginary part of μ given by Eq. (10) with real δ_c in expression (9), we obtain the curves of $\rho_c(T) = 1/\sigma_c(T)$ at $T > T_c$ shown in the right-hand insets to Figs. 6a and 6b for crystals #1 and #2. Further, using the known functions $\sigma_c(T)$ and $\sigma_{ab}(T)$ at $T > T_c$ and substituting the real part μ determined by Eq. (10) in expression (9), we calculate $(-2\delta f/f)$ versus temperature in the normal state, and these calculations are plotted by the solid lines in Fig. 6. These lines are approximately parallel to the experimental curves of $-2\Delta f/f$ in the L-orientation (open circles in Fig. 6). The difference $-2(\delta f - \Delta f)/f$ yields the additive constant f_0. Given f_0 and $\Delta f(T)$ measured in the range $T < T_c$, we also obtain $\delta f(T)$, hence $\mu(T)$, in the superconducting state in the L-orientation. As a result, with due account of $\sigma_{ab}(T)$ in the T-orientation, we obtain the curves $\sigma_c'(T)$ and $\sigma_c''(T)$ of BSCCO #1 and BSCCO #2 crystals shown in Figs. 7a and 7b respectively. In sample #1 the value of $\lambda_c(0)$ proved to be approximately equal to 50 μm and in sample #2 150 μm. These results are in reasonably good agreement with our measurements of $\lambda_c(0)$ in these crystals that were obtained using other techniques[14,15].

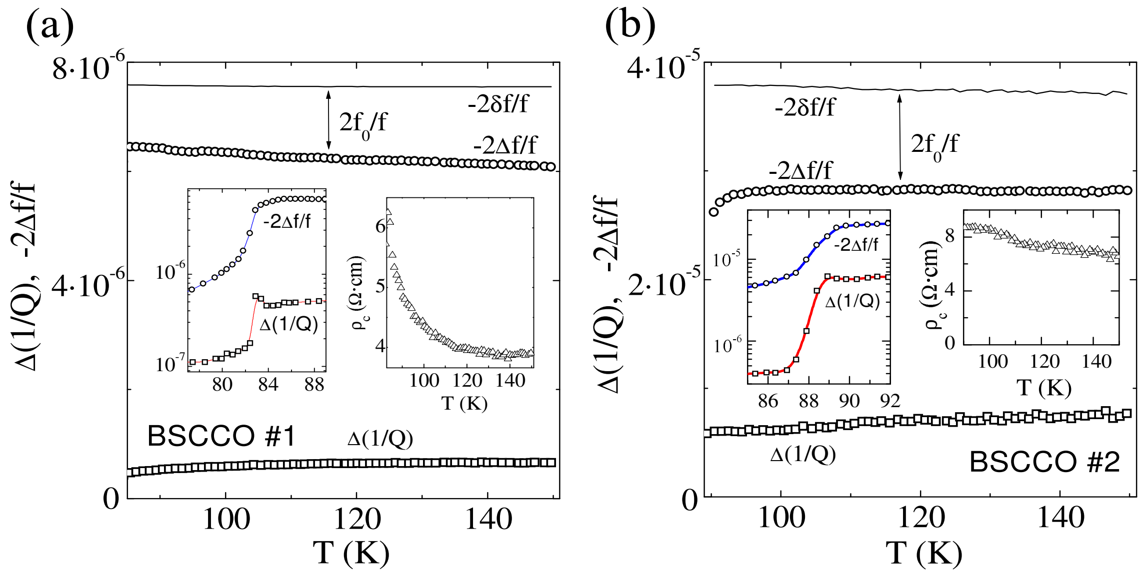

FIG. 6. Temperature dependences of $\Delta(1/Q)$ (open squares) and $-2\Delta f/f$ (open circles) at $\mathbf{H}_\omega \parallel \mathbf{b}$ of sample #1 (Fig. 6a) and sample #2 (Fig. 6b) at $T > T_c$. Solid lines show the functions $-2\delta f(T)/f$ deriving from Eqs. (9) and (10). Left-hand insets: $\Delta(1/Q)$ and $-2\Delta f/f$ as functions of temperature in the neighborhood of T_c. Right-hand insets: $\rho_c(T)$ (triangles).

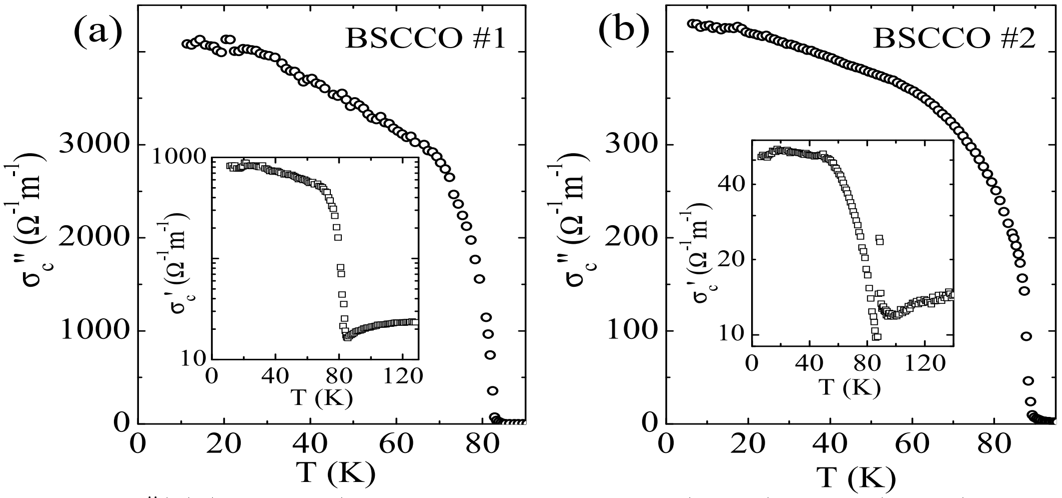

FIG. 7. Conductivities $\sigma_c''(T)$ (open circles) of BSCCO single crystals #1 (Fig. 7a) and #2 (Fig. 7b) at 9.4 GHz, obtained by comparing the measurements of $\Delta(1/Q)$ and $\Delta f = \delta f + f_0$ to numerical calculations by Eqs. (9) and (10). The insets show the behavior of $\sigma_c'(T)$ (open squares).

IV. ANALYSIS OF EXPERIMENTAL RESULTS IN TRANSVERSE ORIENTATION

A. Surface impedance

In the temperature range $T \geq T_c$, $R_s(T) = X_s(T)$ in the ab-plane of BSCCO (Fig. 3)[9,12,16], YBCO[7,16–18] and TBCCO[19] single crystals, and this relation is equivalent to the condition of the normal skin effect. At temperatures higher than T_c in all HTS single crystals, the temperature dependence of $R_s(T)$ is adequately described by the expression $2R_s^2(T)/\omega\mu_0 = \rho_{ab}(T) = \rho_{ab}(0) + bT$. In particular, for the crystal BSCCO #2 (Fig. 3) $\rho_{ab}(0) \approx 13\ \mu\Omega\cdot$cm and $b \approx 0.3\ \mu\Omega\cdot$cm/K.

The issue of the temperature dependence of the impedance of TBCO[20,21] and HgBaCuO crystals[22] raises controversy. The problem is that, even if curves of $R_s(T)$ are matched to curves of $\Delta X_s(T)$ in the range $T \geq T_c$: $R_s(T) = \Delta X_s(T)$, the change in the reactance $\Delta X_s(T)$ in the superconducting region is larger than the change $\Delta R_s(T)$, so that we obtain negative values of $X_s(0)$. The problem is also complicated by the circumstance that the coefficients of thermal expansion for TBCO and HgBaCuO cannot be found in literature. If we assume that the thermal expansion coefficient of TBCO in the range $T > T_c$ equals that of BSCCO[23] or TBCCO[24] and take into account the frequency shift $\Delta f_{th}(T)$ in Eq. (2), the curves of $R_s(T)$ and $X_s(T)$ for TBCO are parallel to one another in the normal state. But the attempt to bring these curves to coincidence so as to satisfy the condition of normal skin effect leads to the value $X_s(0) = \omega\mu_0\lambda_{ab}(0) < 0$. Thus, the problem can be solved by either discovering the cause of the negative contribution $dX_s < 0$ in the range $T < T_c$, which should be subtracted from the measurements of $\Delta X_s(T)$ to obtain true values of the reactance, $X_s(T) > 0$, which equals $R_s(T)$ at $T > T_c$, or explaining the positive difference $X_s(T) - R_s(T)$ in the normal state of TBCO at which a reasonable value of $X_s(0)$ is obtained. A tentative explanation of this discrepancy could be based on two features of the TBCO structure and growth conditions which distinguish this material from BSCCO. It is known that so-called cleavage planes can intersect with the TBCO surfaces, whereas the surfaces of the BSCCO crystals are smooth. If the intersection lines of these planes form juts (grooves) on the crystal surfaces in the form of long lines, and the dimensions of these irregularities (their heights, widths, and periods of their patterns) are larger than the magnetic field penetration depth in the direction perpendicular to the surface, the magnetic field screening by these irregularities brings about a negative contribution $dX_s < 0$[25] to the measured reactance $X_s(T)$. The field penetration depth increases with the temperature, and at a certain temperature $T^* < T_c$ it becomes comparable to the dimensions of these irregularities. Therefore, the contribution dX_s to the reactance can be neglected at $T > T^*$. Another likely cause of the measurements of $X_s(T)$ to be higher than $R_s(T)$ in the normal state of TBCO is the size effect in the T-orientation. Whereas the elementary cell of the BSCCO crystal lattice contains two conducting CuO_2 planes, the elementary cell in TBCO, which has approximately the same dimensions, includes only one. If we assume that dissipative high-frequency currents are induced only in these planes, the screening length c^* in the TBCO crystal should be much smaller than its actual thickness c: $c^* \ll c$. If $c^* < 3\delta_{ab}$, the measured effective parameter $X_s^{eff}(T)$ is larger than the effective $R_s^{eff}(T)$ at $T \geq T_c$ owing to the size effect.

For the frequencies $\lesssim 10$ GHz, the common features of all HTS single crystals are the linear temperature dependence of the surface resistance ($\Delta R_s(T) \propto T$) and of the surface reactance ($\Delta X_s(T) \propto \Delta\lambda_{ab}(T) \propto T$) at temperatures $T \ll T_c$ (see Refs.[1,26–28] and references therein). The slopes of $\Delta\lambda_{ab}(T)$ curves at $T \ll T_c$ are different.

In particular, in YBCO crystals fabricated by different techniques, the slopes of $\Delta\lambda_{ab}(T)$ differ by almost one order of magnitude[18,29,30].

An important parameter of HTS crystals characterizing their quality is the residual surface resistance $R_{res} = R_s(T \to 0)$, which is the loan-term taken from the terminology of conventional superconductors. There is, however, a marked difference between these two cases: whereas R_{res} in conventional superconductors is clearly defined as the level of the plateau on the $R_s(T)$ curve in the region $T < T_c/4$, no plateau has been detected on the characteristic curves of the $R_s(T)$ in HTS, and R_{res} is set to the value $R_s(T=0)$, which is obtained by extrapolating to the zero temperature the linear section of the $R_s(T)$ curve in the region $T \ll T_c$ (Fig. 2). It was found in experiments with conventional superconductors[25] that the parameter $R_{res} \propto \omega^2$ and is determined by various defects in the surface layers of samples, therefore, it is generally accepted that the sample quality is the higher, the lower R_{res}. The residual surface resistance of HTS materials is also proportional to the microwave frequency squared, but its magnitude, even in samples of the highest quality, is a factor of several tens higher than R_{res} of conventional superconductors. If we recall that, in spite of the intense search for new techniques of HTS crystals manufacture during the latest five to seven year, no essential progress has been made, and the characteristic R_{res} has not been reduced notably (moreover, as will be shown in the following sections, the temperature dependence $\sigma'(T)$ in samples of similar chemical compositions is radically different at different R_{res}), it becomes quite clear that the explanation of the nature of residual losses has remained a topical problem in the HTS physics.

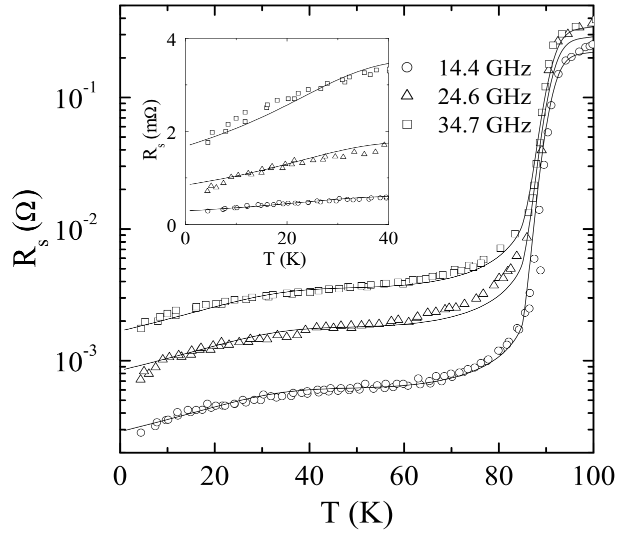

FIG. 8. Experimental data of BSCCO single crystal[37] at various frequencies: 14.4 GHz (circles), 24.6 GHz (triangles) and 34.7 GHz (squares). The solid curves plot the calculated functions $[R_s(T) + R_{res}]$ with R_{res} set to 0.29, 0.85 and 1.7 mΩ, respectively. The inset shows the temperature dependences of the surface resistance at low temperatures.

Let us consider now the differences between the $Z_s^{ab}(T)$ characteristics of BSCCO, TBCCO and TBCO single crystals on the one side, whose lattices are tetragonal, and YBCO crystals with the orthorhombic lattice on the other. Whereas the linear region of $\Delta R_s(T) \propto T$ in the tetragonal materials, obtained at a frequency ~ 10 GHz, can extend to almost $T_c/2$ (Figs. 2, 3, and 8), in YBCO the linear region terminates near or below $T < T_c/3$, and at higher temperatures $R_s(T)$ of YBCO has a broad peak (Fig. 9). The peak shifts to higher temperatures and diminishes in size as the frequency is increased. In higher-quality YBCO crystals the peak amplitude increases and $R_s(T)$ reaches its maximum at a lower temperature[31]. In addition, the $\lambda_{ab}(T)$[18,29] and $R_s(T)$[29] curves of some YBCO single crystals have unusual features in the intermediate temperature range $T \sim T_c/2$.

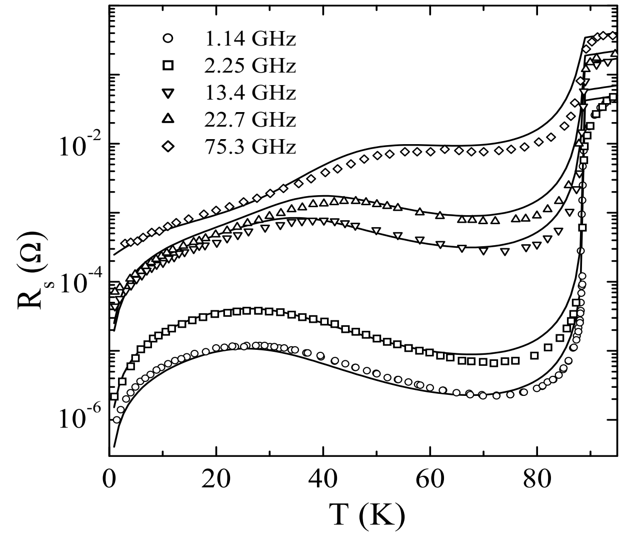

FIG. 9. Comparison between calculated (lines) and measured surface resistance $R_s(T)$ in the ab-plane of YBCO single crystal at 1.14, 2.25, 13.4, 22.7 and 75.3 GHz (symbols) from Ref.[31]. The solid lines are calculations by Eqs. (4), (15), and (16) with parameter $\kappa = 9$ and experimental values $\tau(T_c) = 10^{-13}$ s, $\beta = 0.005$, and $n_s(T)/n = \sigma''(T)/\sigma''(0)$. We assumed $R_{res} = 0.3$ mΩ for 75.3 GHz and zero for all other frequencies.

B. Complex conductivity

The components $\sigma'(T)$ and $\sigma''(T)$ are not measured directly, but can be derived from measurements of $R_s(T)$ and $X_s(T)$ using Eq. (6). At temperatures not very close to T_c, $R_s(T) \ll X_s(T)$ in HTS crystals of high quality, and Eq. (6) reduces to

$$\sigma'(T) = \frac{2\omega\mu_0 R_s(T)}{X_s^3(T)}, \quad \sigma''(T) = \frac{\omega\mu_0}{X_s^2(T)}. \qquad (12)$$

It then follows from Eq. (12) that $\sigma_1/\sigma_2 = 2R_s/X_s \ll 1$ at $T < T_c$. The increments $\Delta\sigma'(T)$ and $\Delta\sigma''(T)$ depend on the increments $\Delta R_s(T)$ and $\Delta X_s(T)$ relative to the respective quantities:

$$\Delta\sigma' \propto \left(\frac{\Delta R_s}{R_s} - 3\frac{\Delta X_s}{X_s}\right), \quad \Delta\sigma'' \propto -\frac{\Delta X_s}{X_s}. \qquad (13)$$

Hence, the curves of $\sigma''(T)$ are determined by the function $X_s(T) = \omega\mu_0\lambda(T)$ alone and reflect the basic properties of the field penetration depth plotted against temperature, namely, its rectilinear shape at low temperatures in all high-quality HTS crystals and the features detected in YBCO in the intermediate temperature range. The behavior of the real part $\sigma'(T)$ of the conductivity, as follows from Eq. (13), is determined by the competition between the relative increments $\Delta R_s/R_s$ and $\Delta X_s/X_s$. In conventional superconductors, the quantity $R_s(T)$ is so small at $T < T_c$ that the increment $\Delta\sigma'(T) > 0$, i.e., the real part of the conductivity increases with the temperature (at least in the temperature interval $T < 0.8T_c$, before the maximum of the BCS coherence peak is reached). For HTS single crystals $\Delta X_s(T) \gg \Delta R_s(T)$ at $T < T_c$. Although $R_s(T) < X_s(T)$, the parameter $\Delta R_s/R_s$ in Eq. (13) can be smaller than $3\Delta X_s/X_s$, and the conductivity $\sigma'_{ab}(T)$ can drop with the temperature: $\Delta\sigma'_{ab}(T) < 0$. This situation occurs in YBCO crystals *a fortiori* since $\Delta R_s/R_s < 0$ on the right-hand slope of the $R_s(T)$ peak. Therefore, starting with $T = 0$, the function $\sigma'(T)$ rises, then it achieves its peak value at a certain $T = T_{max}$, and drops as the temperature increases further, i.e., the curve of $\sigma'(T)$ has a peak at $T < T_c$. It follows from Eq. (13) that this shape of the curve can take place if the value of the residual surface resistance R_{res} is sufficiently small:

$$R_{res} < \frac{X_s(0)}{3}\,\frac{\Delta R_s(T)}{\Delta X_s(T)}\bigg|_{T\to 0}. \qquad (14)$$

The peak of $\sigma'_{ab}(T)$ shifts to lower temperatures (T_{max} drops) as R_{res} increases, and when R_{res} achieves the value on the right of Eq. (14), the peak disappears ($T_{max} = 0$). If R_{res} of the crystal is such that inequality (14) cannot be satisfied any longer, its conductivity $\sigma'_{ab}(T)$ is a monotonically decreasing function of the temperature in the range $T < T_c$. Figures 5a and 5b show the two possible shapes of the $\sigma'_{ab}(T)$ curves measured at a frequency of 9.4 GHz, namely, the presence of the peak in the sample BSCCO #1 (Fig. 5a; $R_{res} \approx 120\ \mu\Omega$) and its absence in BSCCO #2 (Fig. 5b; $R_{res} \approx 500\ \mu\Omega$). The higher the crystal quality, the more clearly the peak in the conductivity at $T < T_c$ can be seen. The curve of $\sigma'_{ab}(T)$ in Fig. 10 corresponds to the characteristic $R_s(T)$ of the YBCO crystal measured at a frequency of 1.14 GHz (Fig. 9) with $R_{res} \sim 1\ \mu\Omega$. Near $T = 0$, $\sigma'(T)$ increases linearly with T and reaches its peak value at T_{max}, which is always higher than the normal state conductivity $\sigma(T_c)$. In YBCO single crystals, the temperature T_{max} is close to the temperature at which the peak of $R_s(T)$ occurs. The peak of $\sigma'_{ab}(T)$ shifts to higher temperatures, and its amplitude diminishes as the microwave frequency increases. At $0.7 < T \le T_c$ the real part of the conductivity does not show a coherence peak, as was predicted by BCS. Usually $\sigma'(T)$ of HTS single crystals has a narrow peak near T_c (Fig. 10), whose width equals the width of the transition from the normal to superconducting state on the curve of $R_s(T)$ at microwave frequencies.

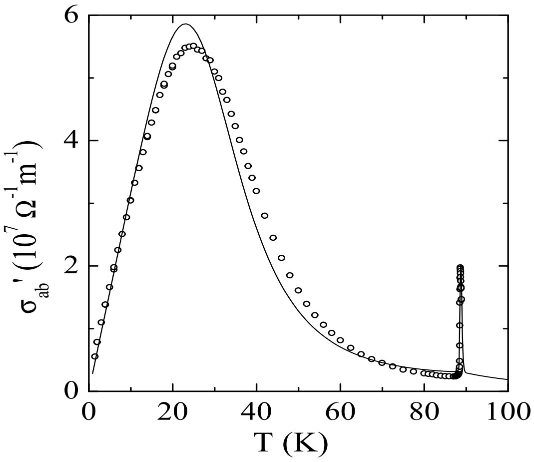

FIG. 10. Real part of the conductivity $\sigma'_{ab}(T)$ of YBCO single crystal at 1.14 GHz[31]. The solid line is the calculated T–dependence of $\sigma'_{ab}(T)$ using Eqs. (15), (17), and (18) with $\kappa = 9$, $\tau(T_c) = 10^{-13}$ s, $\beta = 0.005$ and $\delta T_c = 0.4$ K.

C. Modified two-fluid model

There is a simple description of all the observed features of $Z_s^{ab}(T)$ and $\sigma_{ab}(T)$ which was suggested in Refs.[32,33] and later developed in Refs.[1,27,28,34,35]. The underlying idea was to generalize the two-fluid model by Gorter and Casimir[36] to the case of HTS materials, whose common feature is the high values of T_c. In metals, processes of inelastic scattering of quasiparticles are essential at such high temperatures, therefore the first unquestionable modification of the two-fluid model should be the introduction of a temperature dependence of the 'normal-fluid' quasiparticle relaxation time $\tau(T)$. Assuming that scattering processes in this liquid are similar to those in normal metals, we used the Bloch-Grüneisen formula (electron–phonon interaction) for the function $\tau(T)$ in the normal and superconducting states of HTS and retained the temperature-independent impurity relaxation time $\tau(0)$, which is present in the standard two-fluid model:

$$\frac{1}{\tau} = \frac{1}{\tau(0)}\left[1 + \frac{t^5\mathcal{J}_5(\kappa/t)/\mathcal{J}_5(\kappa)}{\beta}\right], \quad \mathcal{J}_5(\kappa/t) = \int_0^{\kappa/t} \frac{z^5 e^z\,dz}{(e^z-1)^2}, \qquad (15)$$

where $t \equiv T/T_c$, $\kappa = \Theta/T_c$ (Θ is the Debye temperature) and β is a numerical parameter, which equals, as it follows from Eq. (15), $\beta = \tau(T_c)/[\tau(0) - \tau(T_c)]$. Following the formal analogy with metals, one can say that the parameter β is the characteristic of the 'HTS purity': $\beta \approx \tau(T_c)/\tau(0) \ll 1$ if $\tau(0) \gg \tau(T_c)$. The parameter of HTS corresponding to Θ can be estimated as several hundreds of degrees. At $T < \Theta/10$ ($\kappa > 10t$) the second summand in the brackets on the right of Eq. (15) is proportional to T^5; in the region $T > \Theta/5$ ($\kappa < 5t$) it is proportional to T. Thus, if $\beta < 1$ the reciprocal relaxation time (the electron relaxation rate) is constant and equal to $1/\tau(0)$ over the interval $0 < T < T_c/3$, and at higher temperatures it increases gradually, starting as the power function $\propto T^5$ in the region $T < T_c/2$ and switching to $\propto T$ around T_c, and at $T > T_c$ we have a linear dependence $\Delta\rho_{ab}(T) \propto 1/\tau(T) \propto T$.

Even though the chosen form of the function $\tau(T)$ for HTS materials with complex electronic spectra was over-simplified, it turned out that all common and even specific features of the $R_s(T)$ and $\sigma'_{ab}(T)$ curves for both $T < T_c$ and $T > T_c$ are adequately described by the modified two-fluid model with only one fitting parameter κ in (15). Indeed, the components of the complex conductivity are

$$\sigma' = \frac{n_n e^2 \tau}{m} \frac{1}{1+(\omega\tau)^2}, \quad \sigma'' = \frac{n_s e^2}{m\omega}\left[1 + \frac{n_n}{n_s}\frac{(\omega\tau)^2}{1+(\omega\tau)^2}\right] \tag{16}$$

and in the case of $(\omega\tau)^2 \ll 1$, which is typical of HTS crystals at all temperatures in the frequency band about 10 GHz and below, they transform to a very simple form:

$$\sigma' = \frac{n_n e^2 \tau}{m}, \qquad \sigma'' = \frac{n_s e^2}{m\omega}. \tag{17}$$

In (16) and (17) $n_{n,s}(T)$ are the densities of the fractions of normal and superconducting carriers (both have the same charge e and effective mass m). At temperatures $T \le T_c$ the total carrier concentration $n = n_s + n_n$ is equal to the concentration of quasiparticles in the normal state. From measurements of $R_s(T_c)$ and $X_s(0)$, and slopes dR_s/dT and dX_s/dT at $T \ll T_c$, one can easily derive, using formulae (4) and (17), the parameters

$$\omega\tau(T_c) = \frac{X_s^2(0)}{2R_s^2(T_c)} = \frac{\sigma_1(T_c)}{\sigma_2(0)}, \quad \omega\tau(0) = \left.\frac{dR_s}{dX_s}\right|_{T\to 0}$$

and determine the parameter β in Eq. (15). Now, if we use the dependence $n_s(T)/n = \sigma''(T)/\sigma''(0) = \lambda^2(0)/\lambda^2(T)$ determined in the same experiment and thus derive the function $n_n(T)/n = 1 - n_s(T)/n$, we can fit, using Eqs. (15)–(17) and evaluating the parameter κ of the sample, formula (4) to the measurements of $R_s(T)$ given above and then derive the real part of the conductivity $\sigma'_{ab}(T)$ of the HTS crystals in the T-orientation using formula (6). The solid lines in Figs. 5, 8–10 show how the experimental data compare with the calculations by the modified two-fluid model.

Here we have to consider two important points that have not been discussed as yet, but were implicitly used in our calculations. Firstly, near T_c we took into account the inhomogeneous broadening δT_c of the superconducting transition following the approach[2,27,28] that describes a peak of the effective conductivity $\sigma'(T)$ at a temperature $T_m = T_c - \delta T_c$, which is close to the critical temperature. The relative amplitude of this peak, which equals

$$\frac{\sigma'(T_m) - \sigma(T_c)}{\sigma(T_c)} \approx \begin{cases} \gamma & \text{if } \gamma > 1 \\ \gamma^2 & \text{if } \gamma < 0.1 \end{cases} \tag{18}$$

($\gamma = \delta T_c/[T_c\omega\tau(T_c)]$), is the lower, the more narrow the superconducting transition is (the smaller δT_c). Usually microwave experiments yield $\gamma > 1$. In particular, the data published by Hosseini et al.[31] lead to $\gamma \simeq 7$ at 1.14 GHz (Fig. 10), therefore the peak amplitude should be inversely proportional to the frequency. This assertion is supported by the comparison between the curves of $\sigma'_{ab}(T)$ (the lines in Fig. 11) from Ref.[37] obtained at two different frequencies on the same BSCCO crystal as was used in Fig. 8.

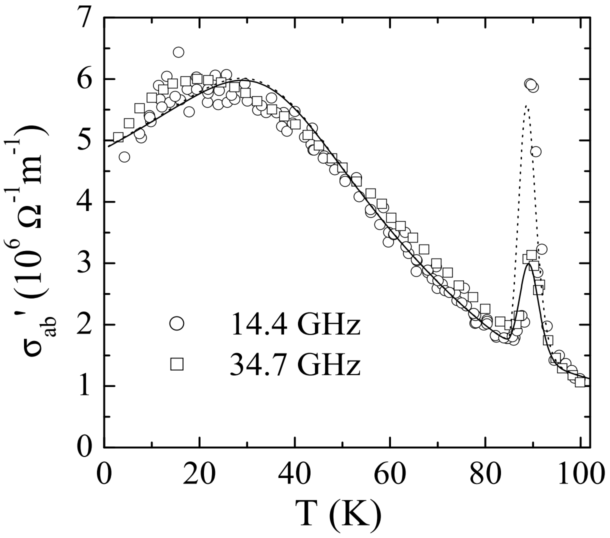

FIG. 11. Measurements of $\sigma'(T)$ of BSCCO single crystal at 14.4 and 34.7 GHz[37] (symbols) and calculations of $\sigma'(T)$ (lines) using Eqs. (15), (17), and (18) with $\kappa = 4$, $\tau(T_c) = 0.8 \cdot 10^{-13}$ s, $\beta = 0.1$, $\delta T_c = 2$ K, R_{res}(14.4 GHz)=0.29 mΩ, R_{res}(34.7 GHz)=1.7 mΩ.

Secondly, in comparing the calculations based on the modified two-fluid model to the measurements of the surface resistance, we added to the function $R_s(T)$ determined by the general formula (4) the value R_{res}, which was determined in the same experiment and is independent of the temperature. For this reason, the curves of $\sigma'_{ab}(T)$ in Figs. 5 and 11, which were calculated by Eq. (6), do not tend to zero as $T \to 0$, even though the carrier density $n_n = 0$ at $T = 0$, according to the two-fluid model, and, as it follows from Eq. (16) or (17), the conductivity should tend to $\sigma(0) = 0$. The parameter R_{res} was not included in formulae (4) and (6) when we compared the data of Fig. 9 (except the upper curve) and of Fig. 10 with calculations because in that case the ratio $R_{res}/R_s(T_c)$ was very small, less than 10^{-3}. In most HTS crystals which were investigated, however, $R_{res}/R_s(T_c) > 10^{-3}$, and at $T \ll T_c$ the effect of the residual surface resistance is quite notable. Another reason for including R_{res} is the increase in the ratio $R_{res}/R_s(T_c) \propto \omega^{3/2}$ with the frequency ω, which proved to be essential when we compared the calculated and experimental curves in Fig. 11 and the upper curve in Fig. 9.

As was noted above, the cause of the residual losses in HTS materials has remained unclear. Some researchers (e.g., Hein et al.[38]) attributed these losses to the presence of a fraction n_0 of carriers that remain unpaired at $T = 0$. The magnitude of R_{res} was estimated by formula (5) with the nonzero conductivity $\sigma'(0) = n_0 e^2 \tau(0)/m$ from Eq. (17). One can easily prove, however, that this approach requires that the calculations of R_{res} should satisfy inequality (14). If the latter condition is not met, which may occur in HTS crystals, as was shown previously (see Fig. 5b), the number n_0 should be larger than the entire concentration n of the carriers.

In developing the traditional approach to the problem, which attributed the residual surface resistance to various imperfections of the surface, the researchers took account of the losses due to weak links[39–41], twinning planes[41,42], clusters with normal conductivity[43], etc. Numerical estimates, however, indicate that the contributions of these mechanisms to the residual surface resistance are much smaller than the measured R_{res} in HTS materials. Moreover, a very remarkable fact is that the residual surface resistance measured at a frequency of 10 GHz was approximately the same, $R_{res} \sim 100\ \mu\Omega$, in all high-quality copper-oxide HTS crystals of different chemical compositions and fabricated by different methods, irrespective of whether they contained twinning planes or not, and whether measurements were performed on freshly cleaved or as-grown surfaces. This fact, apparently, indicates that the residual losses are inherent to all high-quality HTS crystals, and their origin is in the features of their structure, namely, in its conspicuously layered nature. In other words, a fraction of current flowing in the surface layer of an HTS crystal may run through regions of the layer that are in the normal state and have a finite resistivity ρ_n. In the phenomenological model under discussion, this contribution to the resistance can be included in the form of a circuit element ρ_n connected in parallel to the two-fluid circuit characterized by Eq. (17), i.e., a resistor $\rho = 1/\sigma'$ is shunted by a kinetic inductor $l = 1/\omega\sigma''$ (the parallel connection of ρ and l is in conformity with the formula relating the current to the field in the two-fluid model). Obviously, the complex impedance of the circuit consists of the imaginary part $iX_s = i\omega\mu_0\lambda$ at $T < T_c$ and the sum of two real components: R_s from Eq. (5) and $R_0 = \omega^2\mu_0^2\lambda^3/2\rho_{\rm n}$. At $T = 0$, when $R_s(0) = 0$, the latter summand can play the role of the residual resistance R_{res}, which is proportional to ω^2, according to the experimental data. At a frequency of 10 GHz, and at $R_{res} \approx 100\ \mu\Omega$ and $\lambda(0) \approx 0.2\ \mu$m, which are typical parameters of HTS crystals, we obtain $\rho_n(0) \approx 25\ \mu\Omega{\cdot}$cm, which is the quantity typical of normal metals. Our procedure of comparison with the experimental data on $R_s(T)$ also requires that R_0 be independent of the temperature $T \ll T_c$. This is feasible if $\rho_n(T) \propto \lambda^3(T)$, i.e., $\rho_n(T)$ should be a linear function of temperature for $T \ll T_c$: $\rho_n(t) = \rho_n(0)(1+1.5\alpha t)$, where α is the slope of the curve of $\sigma''(t)$ at $t \ll 1$ for a specific HTS sample:

$$\sigma''(t)/\sigma''(0) = \lambda^2(0)/\lambda^2(t) \simeq (1 - \alpha t). \tag{19}$$

One can easily check out that the coefficients $\rho_n(0)$ and $1.5\alpha\rho_n(0)/T_c$ for the sample BSCCO #2 are approximately equal to $\rho_{ab}(0)$ and b in the resistivity $\rho_{ab}(T) = \rho_{ab}(0) + bT$ of this sample in the normal state, i.e., $\rho_n(T) \approx 2R^2(T)/\omega\mu_0$, where $R(T)$ is the extrapolation of the line $R_s(T)$ in the region $T > T_c$ of the normal state in Fig. 3 to the region of the superconducting state, $T < T_c$, down to the point $T = 0$.

It would be natural to complete this presentation of the modified two-fluid model with formulae describing the experimental data on $n_s(T)/n = \sigma''(T)/\sigma''(0)$, which were used in the calculations of the real parts of the impedance and conductivity in the T-orientation of HTS crystals. Several versions of such empirical formulas are given elsewhere[1,27,28,33,34]. Note only that all these formulas are identical with Eq. (19) at $T \ll T_c$ because all curves of $\sigma''_{ab}(T)$ characterizing high-quality HTS crystals have rectilinear shapes in the region of low temperatures.

To sum up, one can describe characteristic features of $Z_s^{ab}(T)$ and $\sigma_{ab}(T)$ curves in high-quality HTS crystals in terms of the modified two-fluid model based on Eqs. (15)–(19). As follows from these equations, at low temperatures, $t \ll 1$, all curves have linear sections, $\sigma' \propto \alpha t/\beta$, since $n_n/n \approx \alpha t$ and $\tau \approx \tau(0) \approx \tau(T_c)/\beta$; $\Delta\sigma'' \propto -\alpha t$; $R_s \propto \alpha t/\beta$, in accordance with Eq. (5); $\Delta X_s \propto \Delta\lambda \propto \alpha t/2$. As the temperature increases, the curve of $\sigma'(t)$ passes through a maximum at $t < 0.5$ if the residual surface resistance is so small that inequality (14) is satisfied. This peak is due to the superposition of two competing effects, namely, the decrease in the number of normal carriers as the temperature decreases, for $t < 1$, and the increase in the relaxation time, which saturates at $t \sim \beta^{1/5}$. If inequality (14) fails, the function $\sigma'(t)$ chandes monotonically with the temperature. The model also accounts for the peculiarities of the surface impedance and complex conductivity at higher temperatures in HTS single crystals manufactured using different techniques. The underlying ideas and results of the modified two-fluid model have been analyzed from the viewpoint of modern microscopic theories of the microwave response of HTS materials in recent publications[27,28].

V. CONDUCTIVITY ALONG C-AXIS

In comparison with the microwave response of the cuprate layers of HTS materials, the data concerning their microwave properties in the direction perpendicular to these layers are scarce. Moreover, the available experimental data are controversial, therefore, any discussion of general regularities in the temperature dependence of the conductivity components in the direction perpendicular to the CuO_2 layers of HTS crystals is premature. In particular, there is no consensus in literature about $\Delta\lambda_c(T)$ at low temperatures. Even in reports on low-temperature properties of high-quality YBCO crystals, which are the most studied objects, one can find both linear, $\Delta\lambda_c(T) \propto T^{6,11}$, and quadratic dependences[44] in the range $T < T_c/3$. In BSCCO materials, the shape of $\Delta\lambda_c(T)$ depends on the level of oxygen doping: in samples with maximal $T_c \simeq 90$ K $\Delta\lambda_c(T) \propto T$ at low temperatures[9,10,12]; at higher oxygen contents (overdoped samples) the linear function $\Delta\lambda_c(T)$[12] transforms to a quadratic one[10]. The common feature of all microwave experiments is that the change in the ratio $\Delta\lambda_c(T)/\lambda_c(0)$ is smaller than in $\Delta\lambda_{ab}(T)/\lambda_{ab}(0)$ because in all HTS $\lambda_c(0) \gg \lambda_{ab}(0)$.

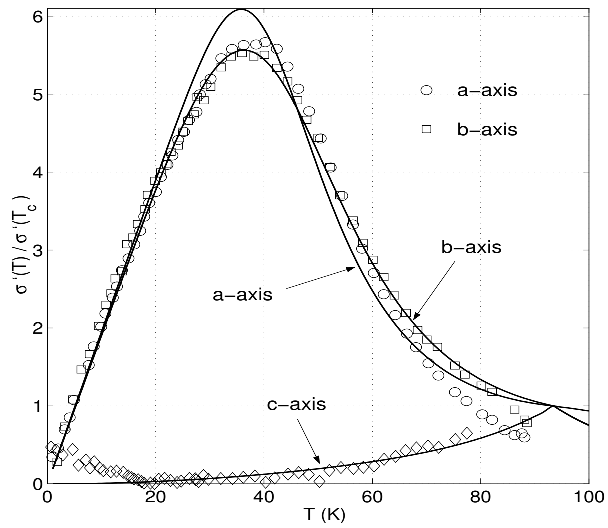

FIG. 12. Real components of the conductivity tensor $\hat{\sigma}'(T)/\sigma(T_c)$ measured along the crystallographic axes of the YBCO crystal at a frequency of 22 GHz[44] at $T < T_c$ (points). The solid lines show calculations by Eqs. (15) and (16) from Ref.[35].

Almost all measurements of losses indicate that $R_s^c(T) \gg R_s^{ab}(T)$ in the superconducting state of HTS. The only exception is the experimental results concerning YBCO crystals with the optimal doping level, which were obtained by Hosseini et al.[44] and demonstrated the opposite relation between these parameters in the region $10 < T < 65$ K. Since measurements of the anisotropy in the cuprate planes of YBCO were also given in that publication, we attempted to apply the modified two-fluid model to the entire set of those experimental data[44]. The calculations of the real components of the conductivity tensor are compared with the experimental data in Fig. 12[35]. The absence of the peak on the curve of $\sigma'_c(T)$ is due to the very weak temperature dependence of the relaxation time of normal quasiparticles in the direction of the c-axis in the region $T < T_c$: $\tau_c(T) \approx$ const, $\beta_c \gg 1$ in Eq. (15). In addition, since the inductive losses (due to large λ_c) are notably higher than the active ones (R_s^c and σ'_c are small), it is plausible that the microwave c-response is largely due to the tunneling of Cooper pairs between the CuO_2 planes. On the other hand, a peak of $\sigma'_c(T)$ at $T < T_c$ was observed in other YBCO crystals with the optimal doping level and the resistance $R_s^c(T) \gg R_s^{ab}(T)^{6,7}$, and this peak was similar to that in $\sigma'_{ab}(T)$.

The conductivity $\sigma'_c(T)$ of BSCCO crystals either drops with the decreasing temperature $T < T_c$[45,46] or rises, as is shown in Fig. 7 for both samples (even though $\sigma'_{ab}(T)$ behaves differently in these two samples, as one can see in Fig. 5). From the formal viewpoint, the cause of this growth is quite clear: the residual losses in the direction of the c-axis of the BSCCO crystals #1 and #2 are fairly high, so inequality (14) fails. The question of what is the nature of these losses has remained unanswered by this time.

VI. CONCLUSION

This paper is an attempt to review the main results and unsolved problems of research into the microwave response of HTS crystals. Measurements of changes in the surface impedance and complex conductivity in the transverse orientation ($\mathbf{H}_\omega \parallel \mathbf{c}$) of samples with different chemical compositions doped to the optimal level could be systematically described in terms of the modified two-fluid model. But even in this specific case, some problems have remained unsolved (in particular, the temperature dependence of the TBCO impedance). One of the topical questions is the cause of residual losses in HTS materials, which determine the behavior of $\sigma'(T)$ in the region $T < T_c$. The experimental technique of measuring all the components of the conductivity tensor is described in detail, and we hope that this technique will be useful in comprehensive studies of anisotropic characteristics of HTS crystals.

VII. ACKNOWLEDGMENTS

I am grateful to my co-authors Herman J. Fink, Yu. A. Nefyodov, and D. V. Shovkun for their help and contribution to this work. Helpful discussions with

A. Agliolo-Gallitto, N. Bontemps, A. Buzdin, V. F. Gantmakher, A.A. Golubov, J. Halbritter, M. Hein, M. Li Vigni, E. G. Maksimov, K. Scharnberg, and S. Sridhar are also acknowledged. This work was supported by RFBR grant 00-02-17053, DFG-RFBR grant 00-02-04021, a grant Coll. Int. Li Vigni, CNRS-RAS 4985, and CLG NATO.

---

[1] M. R. Trunin, Physics–Uspekhi, **41**, 843 (1998); J. Superconductivity **11**, 381 (1998).
[2] M. R. Trunin, A. A. Zhukov, and A. T. Sokolov, JETP **84**, 383 (1997); A. A. Golubov, M. R. Trunin, A. A. Zhukov, O. V. Dolgov, and S. V. Shulga, J. Phys. I France **6**, 2275 (1996).
[3] J. Bardeen, L.N. Cooper, and J.R. Schrieffer, Phys. Rev. **108**, 1175 (1957).
[4] L. D. Landau and E. M. Lifshitz, *Electrodynamics of Continuous Media* (Pergamon, Oxford, 1984).
[5] T. Shibauchi, H. Kitano, K. Uchinokura, A. Maeda, T. Kimura, and K. Kishio, Phys. Rev. Lett. **72**, 2263 (1994).
[6] J. Mao, D. H. Wu, J. L. Peng, R. L. Greene, and S. M. Anlage, Phys. Rev. B **51**, 3316 (1995).
[7] H. Kitano, T. Shibauchi, K. Uchinokura, A. Maeda, H. Asaoka, and H. Takei, Phys. Rev. B **51**, 1401 (1995).
[8] D. A. Bonn, S. Kamal, K. Zhang, R. Liang, and W. N. Hardy, J. Phys. Chem. Solids **56**, 1941 (1995).
[9] T. Jacobs, S. Sridhar, Q. Li, G. D. Gu, and N. Koshizuka, Phys. Rev. Lett. **75**, 4516 (1995).
[10] T. Shibauchi, N. Katase, T. Tamegai, and K. Uchinokura, Physica C **264**, 227 (1996).
[11] H. Srikanth, Z. Zhai, S. Sridhar, and A. Erb, J. Phys. Chem. Solids **59**, 2105 (1998).
[12] D. V. Shovkun, M. R. Trunin, A. A. Zhukov, Yu. A. Nefyodov, H. Enriquez, N. Bontemps, A. Buzdin, M. Daumens, and T. Tamegai, JETP. Lett. **71**, 92, 2000.
[13] C. E. Gough and N. J. Exon, Phys. Rev. B **50**, 488 (1994).
[14] M. R. Trunin, Yu. A. Nefyodov, D. V. Shovkun, A. A. Zhukov, N. Bontemps, H. Enriquez, A. Buzdin, M. Daumens, and T. Tamegai, J. Supercond., to be published.
[15] H. Enriquez, N. Bontemps, A. A. Zhukov, D. V. Shovkun, M. R. Trunin, A. Buzdin, M. Daumens, and T. Tamegai, submitted to Phys. Rev. B.
[16] T. Shibauchi, A. Maeda, H. Kitano, T. Honda, and K. Uchinokura, Physica C **203**, 315 (1992).
[17] D. Achir, M. Poirier, D. A. Bonn, R. Liang, and W. N. Hardy, Phys. Rev. B **48**, 13184 (1993).
[18] M. R. Trunin, A. A. Zhukov, G. A. Emel'chenko, and I. G. Naumenko, JETP Lett. **65**, 938 (1997).
[19] A. A. Zhukov, M. R. Trunin, A. T. Sokolov, and N. N. Kolesnikov, JETP **85**, 1211 (1997).
[20] J. R. Waldram, D. M. Broun, D. C. Morgan, R. Ormeno, and A. Porch, Phys. Rev. B **59**, 1528 (1999).
[21] N. Hakim, Yu. A. Nefyodov, S. Sridhar, and M. R. Trunin, unpublished.
[22] S. Sridhar, private communication.
[23] C. Meingast, A. Junod, and E. Walker, Physica C **272**, 106 (1996).
[24] M. Hasegawa, Y. Matsushita, and H. Takei, Physica C **267**, 31 (1996).
[25] F. F. Mende and A. A. Spitsyn, *Surface impedance of superconductors* (Kiev: Naukova dumka, 1985).
[26] D. A. Bonn and W. N. Hardy, in *Physical Properties of High Temperature Superconductors V*, D. M. Ginsberg, eds. (World Scientific, Singapore, 1995), p.p. 7-97.
[27] M. R. Trunin, Yu. A. Nefyodov, and H. J. Fink, JETP **91**, (2000).
[28] M. R. Trunin and A. A. Golubov, in *HTSC Spectroscopy,* N. M. Plakida, eds. (Gordon and Breach, 2000), to be published.
[29] H. Srikanth, B. A. Willemsen, T. Jacobs, S. Sridhar, A. Erb, E. Walker, and R. Flükiger, Phys. Rev. B **55**, R14733 (1997).
[30] S. Kamal, R. Liang, A. Hosseini, D. A. Bonn, and W. N. Hardy, Phys. Rev. B **58**, 8933 (1998).
[31] A. Hosseini, R. Harris, S. Kamal, P. Dosanjh, J. Preston, R. Liang, W. N. Hardy, and D. A. Bonn, Phys. Rev. B **60**, 1349 (1999).
[32] M. R. Trunin, A. A. Zhukov, G. E. Tsydynzhapov, A. T. Sokolov, L. A. Klinkova, and N. V. Barkovskii, JETP Lett. **64**, 832 (1996).
[33] H. J. Fink, Phys. Rev. B **58**, 9415 (1998).
[34] H. J. Fink and M. R. Trunin, Physica B **284-288**, 923 (2000); H. J. Fink, Phys. Rev. B **61**, 6346 (2000).
[35] H. J. Fink and M. R. Trunin, Phys. Rev. B **62**, 3046 (2000).
[36] C. S. Gorter and H. Casimir, Phys. Z. **35**, 963 (1934).
[37] S-F. Lee, D. C. Morgan, R. J. Ormeno, D. M. Broun, R. A. Doyle, and J. R. Waldram, Phys. Rev. Lett. **77**, 735 (1996).
[38] M. Hein, T. Kaiser, and G. Müller, Phys. Rev. B **61**, 640 (2000).
[39] T. L. Hilton and M. R. Beasly, Phys. Rev. B **39**, 9042 (1989).
[40] A. M. Portis and D. W. Cooke, Supercond. Sci. Technol. **5**, S395, (1992).
[41] J. Halbritter, J. Appl. Phys. **68**, 6315 (1990); **71**, 339 (1992).
[42] O. G. Vendik, A. B. Kozyrev, and A. Yu. Popov, Rev. Phys. Appl. **25**, 255 (1990).
[43] O. G. Vendik, L. Kowalevicz, A. P. Mitrofanov, O. V. Pakhomov, A. Yu. Popov, and T. B. Samoilova, Superconductivity: Physics, Chemistry, Technique **3**, 1573 (1990).
[44] A. Hosseini, S. Kamal, D. A. Bonn, R. Liang, and W. N. Hardy, Phys. Rev. Lett. **81**, 1298 (1998).
[45] H. Kitano, T. Hanaguri, and A. Maeda, Phys. Rev. B **57**, 10946 (1998).
[46] M. B. Gaifullin, Y. Matsuda, N. Chikumoto, J. Shimoyama, K Kishio, and R. Yoshizaki, Phys. Rev. Lett. **83**, 3928 (1999).